Subcritical solution of the Yang-Mills Schrödinger equation in the Coulomb gauge

D. Epple, H. Reinhardt, W. Schleifenbaum
Institut für Theoretische Physik
Tübingen University
Auf der Morgenstelle 14
D-72076 Tübingen
Germany

A.P. Szczepaniak
Physics Department and Nuclear Theory Center
Indiana University, Bloomington, IN 47405, USA.
(Dated: February 2, 2008)

In the Hamiltonian approach to Coulomb gauge Yang-Mills theory, the functional Schrödinger equation is solved variationally resulting in a set of coupled Dyson-Schwinger equations. These equations are solved self-consistently in the subcritical regime defined by infrared finite form factors. It is shown that the Dyson-Schwinger equation for the Coulomb form factor fails to have a solution in the critical regime where all form factors have infrared divergent power laws.

PACS numbers: 11.10Ef,12.38Aw,12.38Cf,12.38Lg

I. INTRODUCTION

Low energy gluon modes are expected to be responsible for the distinctive features of QCD such as confinement or chiral symmetry breaking. Current evidence for gluonic excitations is sparse [1, 2, 3, 4], however new experimental efforts at JLab, PANDA, and BES, through studies of hybrid and glueball spectra are expected to shed more light into the nature of gluonic excitations. It is thus highly desirable to develop a theoretical framework for studies of the Yang-Mills sector that is both: rooted in QCD and practical. Coulomb gauge quantization offers such a framework [5, 6, 7, 8, 9, 10, 11, 12, 13]. Elimination of the longitudinal component of the gauge field by imposing the Coulomb gauge condition, $\boldsymbol{\nabla}\cdot\boldsymbol{A}^a(\boldsymbol{x})$ where a denotes color ($a = 1\cdots N_C^2-1$), leaves only two physical transverse components as independent degrees of freedom. In the functional integral approach, the A_0 component becomes constrained and defines the instantaneous potential of color charge, while in the canonical quantization approach Weyl gauge, $A_0 = 0$, is used and the static potential emerges from the resolution of the Gauss law. In the Coulomb gauge the resulting many-body system of transverse gluons interacting via long-range Coulomb exchange forces can be studied using standard techniques. After ultraviolet (UV) regularization it is possible to introduce an ansatz for the ground state vacuum wave functional in terms of the dynamical gluon variables and optimize it by varying the energy density. In particular with a gaussian ansatz a canonical transformation exists which transforms the gauge fields to the particle representation. These quasi-particles satisfy a dispersion relation with a mass gap that originates from non-perturbative self-interactions mediated by the long range Coulomb potential. The expectation value of the Coulomb potential is computed self-consistently in the same vacuum state, and these self-interactions lead to a strong enhancement of the potential for large separation between localized color charges. For a true linear potential the single quasi-gluon mass becomes infinite which is consistent with what is expected for a confining phase: formation of color states requires infinite energy. In a color singlet combination, however, residual interaction between constituents screens the long range interactions and leads to a finite mass for bound states. A priori, however it is not guaranteed that a particular ansatz for the vacuum wave functional would result not only in qualitative but also in quantitative description of all features of confinements. The gaussian ansatz represents fluctuations around topologically trivial distributions of the gauge field and since topologically nontrivial configurations can also minimize the non-abelian Yang-Mills action, a more complicated vacuum wave functional may be needed to, e.g., reproduce the area law behavior of the spacial Wilson loop [14, 15]. Also, the vacuum expectation value of the Coulomb potential is actually not the same as the energy of the state with static sources. External sources polarize vacuum and lead to string formation for large separations. Thus one should not compare the expectation value of the Coulomb energy to the "Coulomb plus linear" potential from lattice gauge simulations of temporal Wilson loops [16, 17]. Nevertheless, the variational Coulomb gauge approach does reproduce the qualitative features of confinement and studying discrepancies between this approach and lattice results, can improve our understanding of the underlying many-body problem.

In a series of papers we studied solutions of the variational problem for the vacuum and single quasi-particle properties under various approximations [10, 11, 12, 13, 18, 19]. The goal of this paper is to review these results, clarify the differences of the various approaches and resolve some open problems. Ref. [10, 11] and [12, 18] use different ansätze for the wave functions and differ

in the extend to which the curvature in the space of gauge orbits introduced by Coulomb gauge fixing was included. While it was shown that the different ansätze for the variational wave functionals is irrelevant to the order of approximation [13], in particular for the infrared behaviour, the inclusion of the curvature of the space of gauge orbits is crucial for obtaining the correct infrared behaviour. The subject of the present paper is the following: We reconsider the renormalization of the Dyson-Schwinger (DS) equations resulting in the variational approach. In particular, we show that to the order considered all UV-divergencies can be removed by adding appropriate counter terms to the Hamiltonian. While in previous calculations the horizon condition (i.e. an infrared diverging ghost form factor) was either assumed or at least seem to follow from numerical solutions in the present paper we study the coupled DS equations in the subcritical regime abandoning the horizon condition. In particular, we will use the infrared analysis of Ref. [19] to investigate the criticality of the various DS equations, i.e. the disappearance of the solution of the DS equations as the infrared exponents exceed certain critical values. We will find that in the limit of critical coupling where the ghost form factor becomes infrared singular, the DS equation for the Coulomb form factor ceases to have a solution. This explains why no consistent solution for the Coulomb form factor was found when the horizon condition is implemented.

The organization of the paper is as follows: In the following Section we summarize the approximations used in solving Dyson-Schwinger equations of the variational Coulomb gauge problem from earlier analyses. In Section III we derive the DS equations and discuss various renormalization schemes. In Section IV we discuss the infrared (IR) limit of the equations. Numerical results and discussion is presented in Section V. Conclusions and outlook are given in Section VI.

II. VARIATIONAL COULOMB QCD

The set of Dyson-Schwinger (DS) equations for correlation functions describing gluon, ghost and the Coulomb propagators are considered within a variational approximation for the ground state vacuum wave functional. The Yang-Mills Coulomb gauge Hamiltonian $H = H(\boldsymbol{A}, \boldsymbol{\Pi})$ is a function of the transverse gluon field, $\boldsymbol{A}^a(\boldsymbol{x})$ and the conjugated momenta, $\boldsymbol{\Pi}^a(\boldsymbol{x}) = -\boldsymbol{E}^a(\boldsymbol{x})$,

$$[\boldsymbol{A}^a(\boldsymbol{x}), \boldsymbol{\Pi}^a(\boldsymbol{y})] = i\delta^{ab}\delta_T(\boldsymbol{x}-\boldsymbol{y}) \tag{1}$$

with $\delta_T = (\mathbb{1} - \boldsymbol{\nabla}\boldsymbol{\nabla}/\boldsymbol{\nabla}^2)\delta$. In the Schrödinger representation, matrix elements of an operator $\mathcal{O}(\boldsymbol{A}, \boldsymbol{\Pi})$ are given by

$$\langle\Psi'|\mathcal{O}|\Psi\rangle = \int \mathcal{D}A J(A)\Psi'(A)\mathcal{O}\left[A, -i\frac{\delta}{\delta A}\right]\Psi(A)\ . \tag{2}$$

In [10, 11] the variational wave functional $\Psi(A) = \langle A|0\rangle \equiv \Psi_0(\omega_0, A)$ in form of a gaussian ansatz was used,

$$\begin{aligned}\Psi_0(\omega_0, A) &= \exp\left(-\frac{1}{2}\int d\boldsymbol{x}d\boldsymbol{y}\boldsymbol{A}^a(\boldsymbol{x})\omega_0(|\boldsymbol{x}-\boldsymbol{y}|)\boldsymbol{A}^a(\boldsymbol{y})\right)\\ &= \exp\left(-\frac{1}{2}\int \frac{d\boldsymbol{k}}{(2\pi)^3}\boldsymbol{A}^a(\boldsymbol{k})\omega_0(k)\boldsymbol{A}^a(\boldsymbol{k})\right)\\ &\equiv \exp\left(-\frac{1}{2}\int A\omega_0 A\right),\end{aligned} \tag{3}$$

where $\boldsymbol{A}^a(\boldsymbol{k})$ is the Fourier transform of $\boldsymbol{A}^a(\boldsymbol{x})$. The functional integration measure contains the Faddeev-Popov (FP) determinant, $J = \exp Tr\ln(-D\partial)$ where $D(\boldsymbol{x}, a; \boldsymbol{y}, b) = [\delta^{ab}\partial_{\boldsymbol{x}} - g f_{abc}\boldsymbol{A}^c(\boldsymbol{x})]\delta(\boldsymbol{x}-\boldsymbol{y})$ is the covariant derivative in the adjoint representation. It reflects the curvature [12] of the Coulomb gauge field space. In [12] it was proposed to include this curvature in the definition of the vacuum wave functional and use,

$$\Psi(\omega_\alpha, A) = J^{-\alpha}(A)\Psi_0(\omega_\alpha, A) \tag{4}$$

with $\alpha = \frac{1}{2}$, which is the usual ansatz for the "radial" wave function in curvilinear coordinates. In Ref. [13] it was shown that within the one loop approximation the resulting DS equations do not depend on α. We will return to this point below. The specific choice $\alpha = 1/2$ which has the advantage of eliminating J from the integration measure when computing vacuum expectation values (vev).

The DS equations involve expectation values of field operators. The gluon two-point function ($\boldsymbol{\delta}_T(\boldsymbol{k}) = \mathbb{1} - \boldsymbol{k}\boldsymbol{k}/\boldsymbol{k}^2$)

$$\int d\boldsymbol{x}e^{i\boldsymbol{k}\boldsymbol{x}}\langle 0|\boldsymbol{A}^a(\boldsymbol{x})\boldsymbol{A}^b(0)|0\rangle = \frac{\delta^{ab}\boldsymbol{\delta}_T(\boldsymbol{k})}{2\omega(k)} \tag{5}$$

defines the gluon gap function $\omega(k)$, which also relates to the single gluon energy. The instantaneous ghost propagator $d(k)$ (better say ghost two-point correlation function) is defined by

$$\delta^{ab}d(k) = \int d\boldsymbol{x}e^{i\boldsymbol{k}\boldsymbol{x}}\langle 0|\frac{\partial^2}{D\partial}(\boldsymbol{x}, a; 0, b)|0\rangle. \tag{6}$$

The square of the FP operator $-1/(D\partial)$ enters the Coulomb potential. The Coulomb form factor $f(k)$ measures the ratio of the vev of its square to the square of vevs,

$$\delta^{ab}f(k)d^2(k) = \int d\boldsymbol{x}e^{i\boldsymbol{k}\boldsymbol{x}}\langle 0|\left[\frac{\partial^2}{D\partial}\right]^2(\boldsymbol{x}, a; 0, b)|0\rangle. \tag{7}$$

Finally we also consider the expectation value of the curvature [12] defined by

$$\delta^{ab}\boldsymbol{\delta}_T(\boldsymbol{k})\chi(k) = -\frac{1}{2}\int d\boldsymbol{x}e^{i\boldsymbol{k}\boldsymbol{x}}\langle 0|\frac{\delta^2\ln J}{\delta\boldsymbol{A}^a(\boldsymbol{x})\delta\boldsymbol{A}^b(0)}|0\rangle\ . \tag{8}$$

The DS equations for these correlations functions were independently studied in [10, 11] and [12, 21] under different approximation schemes. Below we summarize the

derivation of these equations and comment on differences in their solutions obtained so far. More detailed analysis of the equations is presented in the sections that follow.

The gap equation for the gluon propagator is shown in Fig. 1 and follows from minimizing the energy with respect to the ω_α in Eq. (4),

$$0 = \frac{\delta}{\delta\omega_\alpha(k)}\langle 0|H|0\rangle \tag{9}$$

In Fig. 1 the first two diagrams represent the contribution from the kinetic energy terms which include transverse gluon self-interactions from the chromo-magnetic energy proportional to $\boldsymbol{B}^2$ and from chromo-electric energy which depends on the curvature and is proportional to $J^{-1}\boldsymbol{E}J\boldsymbol{E}$.

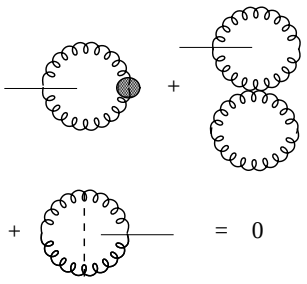

FIG. 1: The gap equation. The diagrams represent vev of the Coulomb gauge Hamiltonian. Thin solid line represent the derivative with respect to ω. The blob represents expectation value of one-body operators, and the dashed line represents the expectation value of the Coulomb potential.

The exchange term represents the contribution from the Coulomb potential which is determined by the expectation value of the Coulomb form factor f and the ghost propagator d. Given ω that solves the gap equation (9), the ghost propagator is computed using Eq. (6) by expanding the inverse of the FP operator in powers of the gluon field and summing all rainbow-ladder diagrams. These are the dominant contributions in the large N_C limit. Corrections to the vertex, coupling the transverse gluon and two ghosts that appears in the expansion of the inverse FP operator were estimated in [10, 19] and found to be small, of the order of $O(10\%)$. We postpone discussion of renormalization to Section III but it is worth noting at this point that in Coulomb gauge this vertex is UV finite. The diagrammatic representation of the DS for the ghost propagator is shown in Fig. 2.

The Coulomb form factor is treated in the same way and the resulting DS equation is shown in Fig. 3. Finally, to the same one-loop order the curvature is given by the loop shown in Fig. 4 that is determined by the product of two ghost propagators arising from the expansion of $\delta^2 \ln J/\delta A\delta A$.

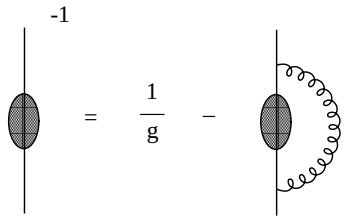

FIG. 2: The DS equation for the ghost propagator, $d(k)$ represented by the oval. The gluon line is represented by the $1/\omega$ propagator.

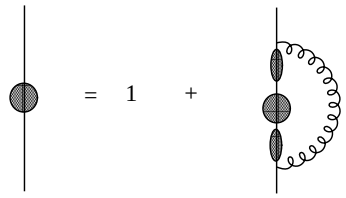

FIG. 3: The DS equation for the Coulomb form factor $f(k)$ represented by the solid circle. The ghost propagator represented by the solid oval and the gluon line is represented by the $1/\omega$ propagator.

The resulting DS equations have a general structure,

$$F[k, f_i(k)] = \int d\boldsymbol{q} K[f_j(\boldsymbol{k}-\boldsymbol{q}), \boldsymbol{k}, \boldsymbol{q}] \tag{10}$$

with f_i being one of the four two-point function (ω,d,f, χ). While χ is merely a definition, ω, d and f obey three coupled DS equations. The main interest is in establishing if these three equations have a common solution and if so what is the momentum dependence of the correlators, especially in the infrared limit. The bare DS equations contain UV divergences and have to be renormalized. Since the variational method does not take into account all diagrams contributing at a given order in the loop expansion removal of ultraviolet divergences requires more than just dimensional transmutation of the coupling constant. Renormalization of the coupling is sufficient to render the ghost propagator finite and thus identifies the ghost propagator with the running coupling. Renormalization of the Coulomb form factor can be accomplished by resealing the Coulomb potential by a renormalization scale dependent constant. The ghost loop is linearly divergent and it turns out that subtraction with a finite residual scale dependence is necessary to render the gap equation finite. Thus renormalization

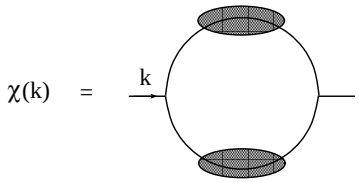

FIG. 4: The one-loop contribution to the FP curvature, $\chi(k)$.

of the curvature introduces a scale in addition to the one defined by the renormalized coupling. As discussed earlier additive change of the curvature is equivalent to a change in ω_α. In particular the inverse gluon propagator is given by [13]

$$\omega(k) = \omega_\alpha(k) + (1-2\alpha)\chi \tag{11}$$

For our preferred choice $\alpha = 1/2$ the wave functional parameter $\omega_{1/2} = \omega(k)$ becomes identical with the inverse of the gluon propagator. It follows from Eq. (11) that a scale-dependent counter-term in χ can be absorbed into ω_α and thus can be interpreted as part of the definition of the variational wave functional ansatz. We discuss this in more detail in the following section. Finally there are quadratic and linear divergences in the gap equations which can be removed by the dimension-2 and dimension-3 counter-terms proportional to $\boldsymbol{A}^2$ and $\{\boldsymbol{A}, \boldsymbol{\Pi}\}$, respectively. To summarize, the variational approach introduced three parameters. One is the scale that can be associated with ω_α as part of the wave functional definition or alternatively it can be associated with χ where it represents finite renormalization. The second is the value of the coupling constant at some arbitrary value of momentum $d(k = \mu_d)$, and third is the value of the Coulomb form factor at an arbitrary value of momentum $f(k = \mu_f)$.

The first study of the DS equations in this framework was carried out in Ref. [10] under the approximation $\chi = 0$, $\alpha = 0$, so that $\omega(k) = \omega_0(k)$. The remaining three equations were solved analytically under angular approximation,

$$|\boldsymbol{k} - \boldsymbol{q}| \to k\theta(k-q) + q\theta(q-k) \tag{12}$$

for the integral on the r.h.s. of Eq. (10). Furthermore, the solution of the gap equation was approximated by $\omega(k) = m_g\theta(m_g - k) + k\theta(k - m_g)$. The effective gluon mass m_g plays the role of the scale parameter discussed above. The solutions for $d(k)$ and $f(k)$ were found to exist for the renormalized coupling $g(\mu) \equiv d(k = \mu)$ less than a critical value. If the renormalization scale is chosen to be m_g then $g(m_g) < 4\pi\sqrt{9/(40N_C)}$. For sub-critical couplings both $f(k)$ and $d(k)$ are finite in the limit $k \to 0$. At the critical coupling $d(k)$ and $f(k)$ diverge as $1/\sqrt{k/m_g}$. Similar behavior of the numerical solutions without angular approximations was also found. For the numerical solutions, however, it could not be verified if in the limit $g \to g_c$ $d(k)$ and $f(k)$ were also IR divergent. This was assumed to be given and accordingly an analytical approximation was proposed. In [11] the effect of the curvature was partially included and a numerical sub-critical solution to all three equations was found (albeit under some approximations to the gap equations). No attempt was made to establish the IR limit nor the value of the critical coupling. At this point it is worth mentioning that the existence of the critical coupling may be an artifact of the variational approximations and the rainbow-ladder approximation. Functional integration over the Coulomb gauge fields ought to be restricted to the fundamental modular region where $Det(-D\partial)$ is positive. In our approximation, however, in each diagram gauge field integration is unrestricted. Thus it is indeed expected that the sum over an infinite set of diagrams, (e.g. of the rainbow-ladder series) converges only in a restricted range of the coupling constant.

The IR behavior of the Coulomb gauge correlators beyond angular approximation and with full inclusion of the curvature was for the first time extensively studied in [12]. There it was found that in the IR the gap equation forces the gluon propagator to have the same momentum behavior as the curvature, $\omega(k) \sim \chi(k)$. Furthermore, under the approximation $f(k) = 1$ it was shown that the gap equation and the ghost DS equation admit a solution with $\omega(k) \to \infty$ as $k \to 0$. Such a solution was not found previously in [10, 11]. In summary, the full set of three DS equations have not been solved so far. The differences in the various solutions currently available may be related to the $f(k) = 1$ approximation (in the IR limit) in [12] or the approximation $\chi = 0$ used in [10], or other approximations made in [11].

In the following we analyze the full set of equations, explain why in [12] it was possible to find an IR vanishing gluon propagator while it was not the case for the solution found in [10, 11], and present a full set of numerical solutions to all three equations.

III. RENORMALIZATION IN THE HAMILTONIAN APPROACH

Each one of the Dyson-Schwinger equations, for the ghost propagator, d, the Coulomb form factor f, the gap equation for ω and the curvature χ requires subtraction of the UV divergences. The gap equation and the Faddeev-Popov determinant contain power divergences and we concentrate on those first.

A. Renormalization of the Faddeev-Popov determinant

Within the approximation we are working the Faddeev-Popov determinant

$$J(A) = Det(-\hat{D}\partial) = \exp\left(Tr\ln(-\hat{D}\partial)\right) \tag{13}$$

can be replaced by [13]

$$J(A) = \exp(-\int A\chi A) \ , \tag{14}$$

i.e. from the Faddeev-Popov determinant mainly the curvature $\chi[\Psi](k)$ enters. Note that the curvature depends on the chosen wave functional Ψ and the representation Eq. (14) can be used only inside the vacuum expectation value (in the state Ψ) and to the considered order (two loops in the energy). From the representation in Eq. (14) it is clear that the counter terms required to renormalize the Faddeev-Popov determinant, or more precisely its logarithm, has to be of the form

$$\sim \int AA \ . \tag{15}$$

Since the log of the Faddeev-Popov determinant can be considered as part of the "action", we renormalize the Faddeev-Popov determinant as

$$\begin{aligned} J \to J\Delta J \ &= \ \exp\left[Tr\ln(-D\partial)\right. \\ &\left. -C_\chi(\Lambda)\int d\boldsymbol{x}\left(\boldsymbol{A}^a(\boldsymbol{x})\right)^2\right] \end{aligned} \tag{16}$$

or by using the representation Eq. (14), we obtain

$$J\Delta J = \exp\left[-\int A\left(\chi - C_\chi(\Lambda)\right)A\right] \ . \tag{17}$$

Obviously the counter term $C_\chi(\Lambda)$ has to be chosen to eliminate the ultraviolet divergent part of the curvature $\chi(k)$. Thus the renormalization condition reads in momentum space

$$\chi(k) - C_\chi(\Lambda) = \ \text{finite} \ . \tag{18}$$

As usual there is some freedom in choosing the finite constants of the right hand side of Eq. (18). In principle, we could just eliminate the ultraviolet divergent part of $\chi(k)$. Since $\chi(k)$ has dimension of momentum and furthermore $\chi(k)$ is linearly divergent in the ultraviolet, it is clear that the ultraviolet divergent part of $\chi(k)$ is given by $\Lambda \cdot const.$. So in principle, we could restrict ourselves to remove just the UV-divergent part of $\chi(k)$ by appropriately choosing the counter term $C_\chi(\Lambda)$. However, it is more convenient to choose $C_\chi(\Lambda)$ to be the curvature at some renormalization scale μ, resulting in the renormalization condition

$$C_\chi(\Lambda) = \chi(\mu) \tag{19}$$

and in the finite renormalized curvature

$$\bar{\chi}(k) = \chi(k) - \chi(\mu) \ . \tag{20}$$

It is easy to check that this quantity is indeed ultraviolet finite and obviously it satisfies the condition

$$\bar{\chi}(k = \mu) = 0 \ . \tag{21}$$

By adopting the renormalization condition Eq. (19) the renormalized quantity $\bar{\chi}(k)$ Eq. (20) depends on the so far arbitrary scale μ. By choosing the renormalization condition Eq. (19) this renormalization scale becomes a parameter of our "model", since it defines the infrared content of the curvature $\chi(k)$, which we keep in the renormalization process, see Fig. 5

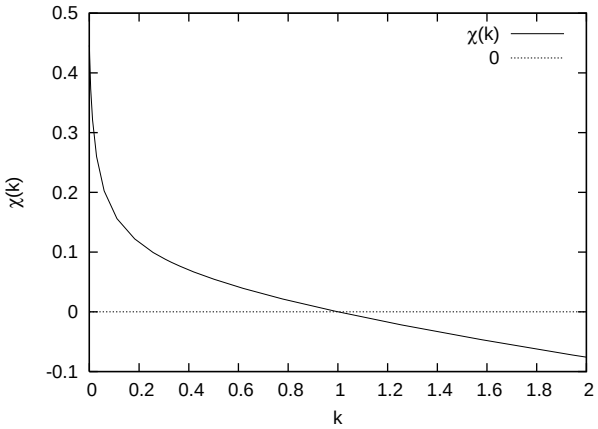

FIG. 5: The scalar curvature. Note the zero of $\bar{\chi}(k)$ at the renormalization scale $\mu = 1$.

If we choose for example $\mu = 0$, we chop off the whole infrared divergent part of the curvature.
In Ref. [18] we have chosen a different renormalization condition keeping from the ultraviolet divergent quantity $\chi(\mu)$ the finite part $\chi'(\mu)$. The renormalized curvature then reads

$$\chi(k) = \bar{\chi}(k) + \chi'(\mu) \ . \tag{22}$$

This implies that we subtract only the divergent part of the curvature keeping fully its finite part. Then we have an extra parameter $\chi'(\mu)$ of the theory and the renormalization scale μ is not related to the zero of the renormalized quantity $\chi(k)$ Eq. (22). Both points of view can be adopted:

1. Using the renormalization condition of Eq. (19) resulting in Eq. (21) and the renormalization scale μ becomes a physical parameter of the theory.

2. Removing only the UV-divergent part of the curvature $\chi(\mu)$ keeping its finite part $\chi'(\mu)$, which is equivalent to choosing the renormalization condition

$$C_\chi(\Lambda) = \chi(\mu) - \chi'(\mu) \ , \tag{23}$$

we obtain an extra finite renormalization parameter $\chi'(\mu)$ and the renormalization scale μ remains arbitrary.

B. Counter terms to the Hamiltonian

According to the general principles of renormalization we should introduce counter terms to the Hamiltonian, calculate the expectation value of the energy and then choose the coefficients of the counter terms such that all divergences disappear from the gap equation. For the Yang-Mills Hamiltonian in Coulomb gauge and the wave functional at hand it turns out the counter terms required are of the form

$$\begin{aligned}\Delta H &= C_0(\Lambda)\int d\boldsymbol{x}\,(\boldsymbol{A}^a(\boldsymbol{x}))^2 \\ &\quad + C_1(\Lambda)\int d\boldsymbol{x}\boldsymbol{A}^a(\boldsymbol{x})\cdot\boldsymbol{\Pi}^a(\boldsymbol{x})\;. \end{aligned} \tag{24}$$

Here the coefficients $C_i(\Lambda), i=0,1$ depend on the momentum cutoff Λ and have to be adjusted so that the UV-singularities in the gap equation disappear. Note also that these coefficients multiply ultralocal operators which are singular in quantum field theory.
We will assume the wave functional of Eq. (4) with $\alpha = 1/2$, as in [12]. For this wave functional the expectation value of the counter term Eq. (24) is given by

$$\begin{aligned}\Delta E &= C_0(\Lambda)\frac{1}{2}t_{ii}\delta^{aa}\int d^3\boldsymbol{x}\omega^{-1}(\boldsymbol{x},\boldsymbol{x}) \\ &\quad + iC_1(\Lambda)\int d^3\boldsymbol{x}\langle\boldsymbol{A}^a(\boldsymbol{x})\cdot\tilde{\boldsymbol{\Pi}}^a(\boldsymbol{x})\rangle_\omega\;, \end{aligned} \tag{25}$$

where $\langle\dots\rangle_\omega$ denotes the expectation value in the Gaussian wave functional with kernel $\omega=\omega_{1/2}$ and

$$\tilde{\boldsymbol{\Pi}}^a(\boldsymbol{x}) = J^{\frac{1}{2}}\boldsymbol{\Pi}^a(\boldsymbol{x})J^{-\frac{1}{2}} = \boldsymbol{\Pi}^a(\boldsymbol{x}) - \frac{1}{2}\left(\boldsymbol{\Pi}^a(\boldsymbol{x})\ln J\right)\;. \tag{26}$$

In Ref. [12] it was shown

$$\begin{aligned}&\langle\boldsymbol{A}^a(\boldsymbol{x})\cdot\tilde{\boldsymbol{\Pi}}^a(\boldsymbol{x})\rangle_\omega \equiv i\langle\boldsymbol{A}^a(\boldsymbol{x})\cdot\boldsymbol{Q}^a(\boldsymbol{x})\rangle_\omega \\ &= i\int d\boldsymbol{x}_1\omega^{-1}(\boldsymbol{x},\boldsymbol{x}_1)\left(\omega(\boldsymbol{x}_1,\boldsymbol{x})-\chi(\boldsymbol{x}_1,\boldsymbol{x})\right)\delta^{aa}\end{aligned} \tag{27}$$

where $\chi(k)$ is the curvature and $\delta^{aa}=N_C^2-1$. In momentum space we find then for the expectation value of the counter terms (25)

$$\begin{aligned}\Delta E &= \left(N_C^2-1\right)V\left[C_0(\Lambda)\int\frac{d\boldsymbol{k}}{(2\pi)^3}\frac{1}{\omega(k)}\right. \\ &\quad \left. -C_1\int\frac{d\boldsymbol{k}}{(2\pi)^3}\frac{\omega(k)-\chi(k)}{\omega(k)}\right]\;. \end{aligned} \tag{28}$$

Taking the variation of this expression with respect to $\omega(k)$ we obtain

$$\begin{aligned}\frac{\delta\Delta E}{\delta\omega(k)} &= \left(N_C^2-1\right)\frac{V}{(2\pi)^3} \\ &\quad \left[-C_0(\Lambda)\frac{1}{\omega^2(k)} - C_1(\Lambda)\frac{\chi(k)}{\omega^2(k)}\right]\;. \end{aligned} \tag{29}$$

Note that $\chi(k)$ depends only on the ghost propagator but not on the gluon gap function ω, at least as long as $\chi(k)$ is not yet the self-consistent solution.
Variation of the expectation value of the energy (without counter terms) yields

$$\begin{aligned}\frac{\delta E}{\delta\omega(k)} &= \frac{N_C^2-1}{2}\delta^3(0) \\ &\quad\times\;\frac{1}{\omega^2(k)}\left[-k^2+\omega^2(k)-\chi^2(k)-I_\omega^0-I_\omega(k)\right], \end{aligned} \tag{30}$$

where $\delta^3(0)=\frac{V}{(2\pi)^3}$ and all other quantities are defined in Ref. [12]. Adding the counter terms from Eq. (28) to the energy we obtain the gap equation

$$\begin{aligned}\omega^2(k) &- \chi^2(k) = \\ &= k^2 + I_\omega^0 + I_\omega(k) - 2C_0(\Lambda) - 2C_1(\Lambda)\chi(k). \end{aligned} \tag{31}$$

C. Renormalization of the gap equation

We now turn to the renormalization of the gap equation (31), which includes already the counter terms. After the renormalization of the Faddeev-Popov determinant, the curvature $\chi(k)$ can be replaced by the renormalized one $\bar\chi(k)$, Eq. (20). Note that the Coulomb integral $I_\omega(k)$ does not depend on any constant part of the curvature, so that $\chi(k)$ could have been replaced right away by the finite quantity $\bar\chi(k)$, Eq. (20). Replacing $\chi(k)$ by $\bar\chi(k)$ and using the relation, see Ref. [12]

$$I_\omega(k) = I_\omega^{(2)}(k) + 2\bar\chi(k)I_\omega^{(1)}(k)\;, \tag{32}$$

the gap equation in Eq. (31) becomes

$$\begin{aligned}&\omega^2(k)-\bar\chi^2(k) = \\ &= k^2 + I_\omega^0 + I_\omega^{(2)}(k) - 2C_0(\Lambda) + 2\bar\chi(k)\left(I_\omega^{(1)} - C_1(\Lambda)\right)\end{aligned} \tag{33}$$

The integrals $I_\omega^{(n=1,2)}(k)$ are linearly ($n=1$) and quadratically ($n=2$) UV-divergent and are defined in [12]. Furthermore, the integral I_ω^0 is also quadratically divergent but independent of the external momentum. We can therefore eliminate all UV-divergences by choosing $C_0(\Lambda)\sim\Lambda^2$ and $C_1(\Lambda)\sim\Lambda$. In principle, the coefficients of the counter terms, $C_i(\Lambda), i=0,1$, have to be

chosen to eliminate the UV-divergent parts of the quantities appearing in the gap equation. This means that we should choose the infinite coefficients $C_i(\Lambda), i = 0.1$ as

$$\left(I^0_\omega + I^{(2)}_\omega(k)\right)\Big|_{\text{UV-divergent part}} - 2C_0(\Lambda) \;=\; 0 \tag{34}$$

$$I^{(1)}_\omega(k)\Big|_{\text{UV-divergent part}} - C_1(\Lambda) \;=\; 0. \tag{35}$$

Note that the UV-divergent parts of $I^{(n=1,2)}_\omega(k)$ are by dimensional arguments independent of the external momentum k. Technically it is more convenient to choose the following alternative renormalization conditions. As usual we have the freedom in choosing the renormalization conditions up to finite constants. Given the fact that I^0_ω is independent of the external momentum and the differences

$$\Delta I^{(n)}_\omega(k,\nu) = I^{(n)}_\omega(k) - I^{(n)}_\omega(\nu) \tag{36}$$

are UV-finite, we can eliminate all UV-divergences by choosing the renormalization conditions

$$I^0_\omega + I^{(2)}_\omega(k=\nu) - 2C_0(\Lambda) \;=\; 0 \tag{37}$$

$$I^{(1)}_\omega(k=\nu) - C(\Lambda) \;=\; 0\,, \tag{38}$$

where ν is an arbitrary renormalization scale, which could be chosen to be the same scale μ of the renormalization of the curvature, but given the fact that with the renormalization presciption Eq. (19), the scale μ becomes a physical parameter, the two renormalization parameters ν and μ need not necessarily be the same. With the renormalization conditions Eqs. (37,38) the renormalized (finite!) gap equation reads

$$\omega^2(k) - \bar\chi^2(k) = k^2 + \Delta I^{(2)}_\omega(k,\nu) + 2\bar\chi(k)\Delta I^{(1)}_\omega(k,\nu) \tag{39}$$

Assuming that the integrals $I^{(n=1,2)}_\omega(k)$ are infrared finite and furthermore that the renormalized curvature $\bar\chi(k)$ is infrared divergent, the infrared limit of the renormalized gap equation is given by

$$\lim_{k\to 0}\left(\omega(k) - \bar\chi(k)\right) = \Delta I^{(1)}_\omega(k=0,\nu)\,. \tag{40}$$

To get the perimeter law of the 't Hooft loop requires that the quantity on the right hand side of Eq. (40) vanishes. This compells us to choose the, in principle, free renormalization parameter ν as $\nu = 0$ [18]. With this choice the renormalized gap equation becomes

$$\omega^2(k) - \bar\chi^2(k) = k^2 + \Delta I^{(2)}_\omega(k,0) + 2\bar\chi(k)\Delta I^{(1)}_\omega(k,0). \tag{41}$$

The coupled DS equations then contain the following so far undetermined parameters: the renormalization scale μ of the renormalization of the curvature and the renormalization constants of the ghost and Coulomb form factors, the former one is fixed by the horizon condition.

D. Renormalization of the ghost and Coulomb form factor

The Dyson-Schwinger equation for the ghost propagator, d is given by [12]

$$\frac{1}{d(k)} = \frac{1}{g} - \frac{N_C}{2}\int d\boldsymbol{l}\frac{1-(\hat{\boldsymbol{l}}\cdot\hat{\boldsymbol{k}})^2}{\omega(l)}\frac{d(\boldsymbol{l}-\boldsymbol{k})}{(\boldsymbol{k}-\boldsymbol{l})^2} \tag{42}$$

and is renormalized by noticing that it corresponds to a running coupling. Regularizing the $\boldsymbol{l}$ integral in the UV by a cutoff Λ and replacing $g \to g(\Lambda)$ leads to a finite equation for d. It is convenient to renormalize d at an IR rather than UV scale which can be done by subtraction,

$$\frac{1}{d(k)} = \frac{1}{d(\mu)} \;-\; \left[\frac{N_C}{2}\int d\boldsymbol{l}\frac{1-(\hat{\boldsymbol{l}}\cdot\hat{\boldsymbol{k}})^2}{\omega(l)}\frac{d(\boldsymbol{l}-\boldsymbol{k})}{(\boldsymbol{k}-\boldsymbol{l})^2} \;-\; (k\to\mu)\right]\,. \tag{43}$$

The Dyson equation for the Coulomb form factor is given by

$$f(k) = Z_f + \frac{N_C}{2}\int d\boldsymbol{l}\frac{1-(\hat{\boldsymbol{l}}\cdot\hat{\boldsymbol{k}})^2}{\omega(l)}\frac{d^2(\boldsymbol{l}-\boldsymbol{k})f(\boldsymbol{l}-\boldsymbol{k})}{(\boldsymbol{k}-\boldsymbol{l})^2}\,. \tag{44}$$

Here $Z_f = Z_f(\Lambda)$ is a Coulomb kernel renormalization constant and the equation renormalized at an IR scale μ is given by

$$f(k) = f(\mu) \;+\; \left[\frac{N_C}{2}\int d\boldsymbol{l}\frac{1-(\hat{\boldsymbol{l}}\cdot\hat{\boldsymbol{k}})^2}{\omega(l)}\frac{d^2(\boldsymbol{l}-\boldsymbol{k})f(\boldsymbol{l}-\boldsymbol{k})}{(\boldsymbol{k}-\boldsymbol{l})^2} - (k\to\mu)\right]\,. \tag{45}$$

IV. INFRARED ANALYSIS AT CRITICAL COUPLING

Here, it is shown that, within the approximations made, there exists no simultaneous solution to the integral equations for d, ω, and f at critical coupling for which the ghost form factor becomes infrared divergent. We first present a simultaneous solution of the integral equations for the ghost form factor $d(p)$ and the Coulomb form factor $f(p)$ as defined above in Eqs.(43), (45). The result obtained is not compatible with the solution obtained by simultaneous treatment of ghost and gluon DS equations found in [19]. We want to check if there are solutions of the Dyson equations for $\omega(p)$, $d(p)$ and $f(p)$ with the ghost form factor $d(p)$ being IR enhanced. To this end, we set for $p \to \infty$

$$\frac{1}{2}\omega^{-1}(p) = \frac{A}{(p^2)^{1+\alpha_Z}}, d(p) = \frac{B}{(p^2)^\kappa}, f(p) = \frac{C}{(p^2)^{\alpha_f}}\,, \tag{46}$$

and $\kappa > 0$ from the horizon condition. By means of the ghost DS equation given in Eq. (43) one can relate the infrared exponent of the gluon to that of the ghost,

$$\alpha_Z + 2\kappa = \frac{d-4}{2} \tag{47}$$

in $d+1$ dimensional Coulomb gauge YM theory. Thus, we eliminate α_Z in favor of κ. Using the infrared integral approximation, we derive from Eq. (43) that [19]

$$(p^2)^{\kappa} = (p^2)^{\kappa} AB^2 N_c I_G(\kappa) \tag{48}$$

becomes exact for $p \to 0$, where

$$I_G(\kappa) = -\frac{4^{\kappa}(d-1)}{(4\pi)^{d/2+1/2}} \frac{\Gamma(\frac{d}{2}-\kappa)\,\Gamma(-\kappa)\,\Gamma(\frac{1}{2}+\kappa)}{\Gamma(\frac{d}{2}-2\,\kappa)\,\Gamma(1+\frac{d}{2}+\kappa)}. \tag{49}$$

Furthermore, we can infer from Eq. (48) that

$$AB^2 N_c I_G(\kappa) = 1 \tag{50}$$

has to hold. Simultaneously solving the gluon DS equation with ω dominated by the curvature $\chi(p)$ in the infrared [12] we find for $d = 3$ exactly two solutions that comply with the horizon condition [19, 20],

$$\kappa \in \left\{0.398, \frac{1}{2}\right\}. \tag{51}$$

Both of these solutions have been found numerically in refs. [12] and [21], respectively.

We now aim at a solution for the Coulomb form factor DS equation given by Eq. (45). For $p \to 0$, one finds

$$(p^2)^{-\alpha_f} = (p^2)^{-\alpha_f} AB^2 N_c I_f(\kappa, \alpha_f) \tag{52}$$

where

$$I_f(\kappa,\alpha_f) = \frac{(d-1)\kappa}{(4\pi)^{d/2}} \frac{\Gamma\left(\alpha_f\right)\Gamma\left(2\kappa\right)\Gamma\left(d/2-2\kappa-2\alpha_f\right)}{\Gamma\left(d/2-2\kappa\right)\Gamma\left(d/2-\alpha_f+1\right)\Gamma\left(\alpha_f+2\kappa+1\right)}. \tag{53}$$

From Eq. (52) we can see that

$$AB^2 N_c I_f(\kappa, \alpha_f) = 1 \tag{54}$$

has to be fulfilled. The above relation from the Coulomb form factor DS equation can now be plugged into the relation Eq. (50) from the ghost DS equation to find

$$I_G(\kappa) = I_f(\kappa, \alpha_F). \tag{55}$$

We now specify the spatial dimension d. For $d = 3$, Eq. (55) yields

$$1 = \frac{(-1+2\,\kappa)\,\cos(\pi\,(\alpha_f+2\,\kappa))\,\Gamma(4-2\,\alpha_f)\,\Gamma(-2\,\kappa)\,\Gamma(1+2\,\alpha_f+4\,\kappa)\,\sin(\pi\,\alpha_f)}{\pi\,(-1+\alpha_f)\,(3+2\,\kappa)\,(-1+2\,\alpha_f+4\,\kappa)\,\Gamma(2+2\,\kappa)}. \tag{56}$$

The numerical solution to this equation gives κ as a function of α_f, as shown in Fig. 6. One can see immediately that for any value of α_f, the ghost exponent κ yields

$$\kappa < \frac{1}{4}. \tag{57}$$

Therefore, recalling the result Eq. (51), there exists no value of α_f for which all three DS equations are satisfied. It is instructive to focus on the case where

$$\alpha_f + 2\kappa = 1 \tag{58}$$

since this leads directly to a linearly rising potential for static quarks. Plugging this constraint into Eq. (56), we find

$$1 = \frac{-2\,\kappa\,(3+2\,\kappa)\,\cos(2\,\pi\,\kappa)\,\Gamma(-1-4\,\kappa)\,\Gamma(1+2\,\kappa)}{(-1+2\,\kappa)\,\Gamma(-1-2\,\kappa)} \tag{59}$$

which has the numerical solution $\kappa = 0.245227$. Surprisingly, this result is exactly agreed upon by lattice calculations [22], where $\kappa = 0.245(5)$ was found. However, one should notice that the lattice calculations carried out so far in Coulomb gauge and also in Landau gauge use too small lattice to give reliable results in the infrared.
In 2+1 dimensions, the calculations are equivalent. From a simultaneous treatment of the ghost DS equation and the gluon DS equation we find for the assumptions that the curvature dominates the infrared a unique solution for the ghost exponent [20],

$$\kappa = \frac{1}{5}. \tag{60}$$

Note that with angular approximation the result is $\kappa = 1/4$. In a recent publication [23], this value for κ was confirmed numerically. On the other hand, if we consider only the ghost DS equation and the equation for the

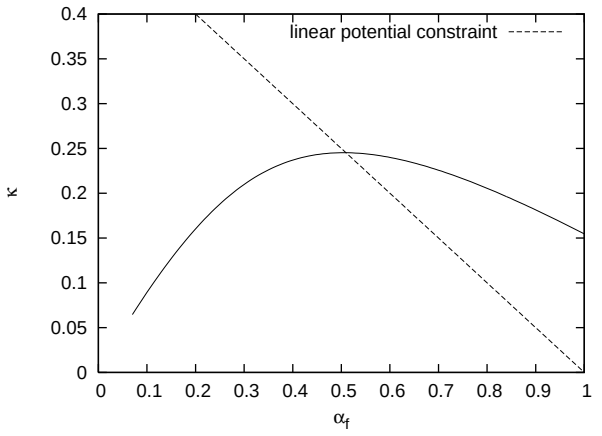

FIG. 6: The ghost exponent κ as a function of α_f is shown by a solid line for $3+1$ dimensions. As a dashed line, it is indicated for which values a linear potential will arise.

Coulomb form factor, see Eqs. (43) and (45) for $d = 2$, one gets by enforcement of the condition Eq. (55):

$$\frac{\Gamma(\alpha_f)\,\Gamma(1-\alpha_f-2\,\kappa)\,\Gamma(\kappa)\,\Gamma(2+\kappa)}{\Gamma(2-\alpha_f)\,\Gamma(-\kappa)^2\,\Gamma(1+\alpha_f+2\,\kappa)} = 1\,. \qquad (61)$$

The numerical solution is shown in Fig. 7. If we require the potential to be linearly rising, the solution has to obey $\alpha_f + 2\kappa = \frac{1}{2}$. Eq. (61) then leads to the numerical value of $\kappa = 0.138$. Lattice results do not agree with this value [24], although they do for $3+1$ dimensions.

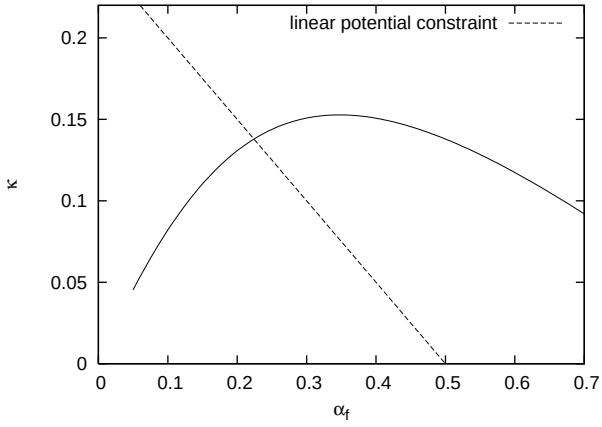

FIG. 7: Same as Fig. 6, here in $2+1$ dimensions.

It is interesting to note that, leaving the DSE for ω aside, a restriction on the infared exponents (57) arises from self-consistency of the equations for d and f only. This restriction also concerns the infrared behaviour of ω via the sum rule (47). Consider a fixed wave functional with a kernel ω that yields $\kappa > \frac{1}{4}$ by its infrared behaviour. In principle, it should be possible to calculate d and f for such a wave functional. However, due to the restriction (57), no solution can be found. We therefore conclude that the Eq. (57) must be due to the approximations made in the DSEs for d and f. Nevertheless, let us stick to the approximation scheme here and investigate whether the relaxation of the horizon condition allows for a self-consistent solution of all DSEs.

V. FULL SUBCRITICAL SOLUTIONS

For the IR analysis given above it follows that the Dyson-Schwinger equations, emerging from the minimization of the vacuum energy functional do not admit coupled solutions with all the functions being IR enhanced. Therefore in the following we do not implement the horizon condition, but rather chose an infrared finite ghost propagator. This allows us to include the ghost propagator fully in the equation for the Coulomb form factor.

Technically, the system is solved in the same way as described in [18, 21], except for the following differences. First, the finite renormalization constant d_0^{-1} is implemented. Then, the infrared extrapolations of the form factors no longer can be done using power law ansätze, since the form factors are all infrared finite. Instead, we approximate the form factors using ansätze of the form

$$d_{\rm ext}(k\to 0) = \frac{1}{k^\beta/B + b} \qquad (62)$$

where β, B and b are parameters and extracted using least-squares fitting. One sees immediately that this ansatz corresponds to the previous ansatz $Bk^{-\beta}$, see (46), if one sets $b = 0$, and that with a finite b we get for the infrared limit of this extrapolating ansatz

$$\lim_{k\to 0} d_{\rm ext}(k\to 0) = \frac{1}{b}, \qquad (63)$$

which means that the fit parameter b corresponds to the renormalization parameter d_0^{-1}. It can serve as a check that the resulting fit parameter b actually turns out to be (numerically) equal to the (input) renormalization parameter d_0^{-1}.

If not stated otherwise below, the other renormalization parameters are chosen as $\mu = 1$, $f_\mu = 1$. Physical units are not available yet in a strict sense, since the usual method of adjusting the Coulomb string tension to its physical value can not be employed here, since the resulting quark-antiquark potential is not linearly rising. This is a direct consequence of the finite renormalization constant d_0^{-1}.

Ansätze of the same form like (62) are then employed for the infrared extrapolations of the other form factors $\chi(k)$, $f(k)$, $\omega(k)$. We chose to use the same ansätze here because the numerically obtained values of the form factors can be approximated by this ansatz pretty well. Of course, every form factor has its own set of fitting parameters. Also $\chi(k)$ and $\omega(k)$ are fitted separately (instead of using a single fit with the combined data, as it has been successful in solving the system with the horizon condition).

A. The search for the critical $d(0)$

First, we searched for the maximal value of $d(0)$ for which the system still has a solution. If one could carry this value to infinity, one had again the horizon condition. It is known from the analytical calculations that the system, however, has no consistent solution, once the horizon condition is enforced. Thus, we expect the system to have a solution only for values of $d(0)$ smaller than some critical value.

Results are presented in Figs.8-13. In Fig. 8, we show the ghost form factor $d(k)$. One finds that the numerical solutions actually show the desired behavior in the infrared, that the infrared fixpoint is at the value of the renormalization constant d_0^{-1}. In Fig. 9, we show the Coulomb form factor $f(k)$. One finds that with larger and larger values of d_0, the Coulomb form factor $f(k)$ becomes more and more enhanced. This has some limit, though, as it is not possible to obtain a solution for arbitrary small values of d_0^{-1}. Furthermore, as the Coulomb form factor gets more and more enhanced, it becomes negative for large momenta. This behavior is not desireable. This fact does not seem to depend sensitively on $f(\mu)$. The largest $d(0)$ where both $f(k)$ is positive for all k and the solution for $d(k)$ is stable has been found to be $d_0^{-1} \approx 0.02$.

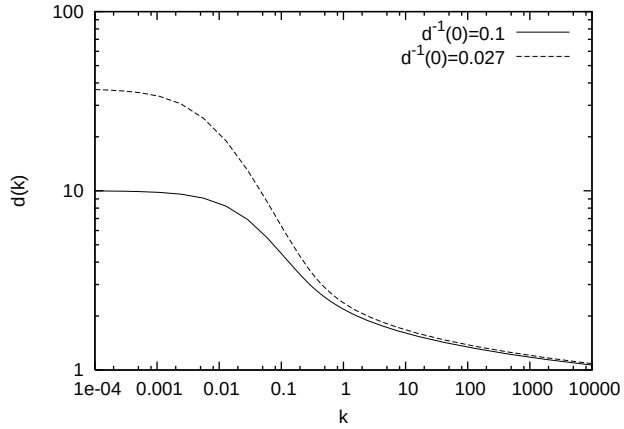

FIG. 8: The ghost form factor $d(k)$.

In Fig. 10 we show the results for $\omega(k)$ and $\chi(k)$. We find that these are infrared finite (perhaps with logarithmical corrections), and not diverging like a power law, as it was found when using the horizon condition.

We have stressed so far the new infrared behavior of the solutions. As shown in Figs. 12 and 13, the ultraviolet behaviour is the same as in the case with the horizon condition implemented. (However, these results are hard to compare, since the results with the horizon condition were obtained using different equations, which use the bare ghost propagator in the Coulomb equation, see above.)

Furthermore, we take a look at the product $d^2(k)f(k)$, see Fig. 14, which is related to the static quark potential

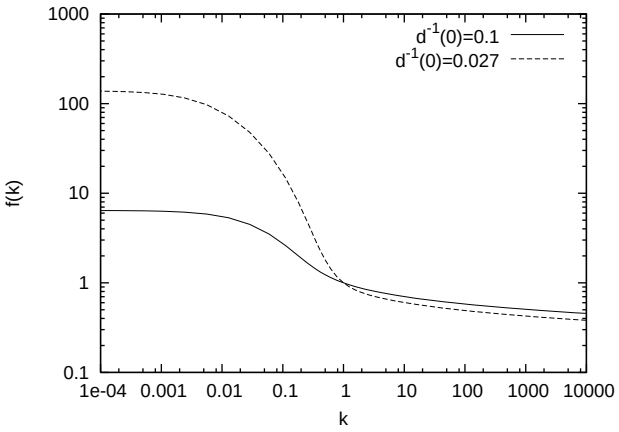

FIG. 9: The Coulomb form factor $f(k)$.

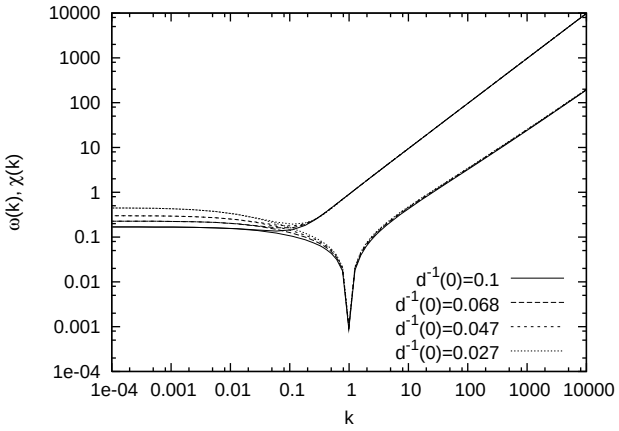

FIG. 10: The gluon energy $\omega(k)$ and the modulus of the scalar curvature, $|\chi(k)|$. The scalar curvature $\chi(k)$ is positive in the infrared, negative in the ultraviolet, such that in the log-log-plot, it seems like it has a pole at its zero.

in momentun space $V(k)$,

$$d^2(k)f(k) \equiv V(k)k^2 \,. \tag{64}$$

Thus, $d^2(k)f(k) \sim 1/k^2$ corresponds to $V(k) \sim 1/k^4$, which after Fourier transform yields a linearly rising quark potential. What one finds in the numerical results is, of course, that the static quark potential saturates for large distances, which stems from the fact that both $d(k)$ and $f(k)$ are infrared finite, but interesting is the feature that for a large momentum range, $d^2(k)f(k)$ actually roughly behaves like $1/k^2$, which results in a linear potential for a large range of distances. We may then assume the slope of this linear part as Coulomb string tension and introduce a physical scale this way. In Fig. 15 the result of $V(k)$ in physical units that were introduced this way is shown.

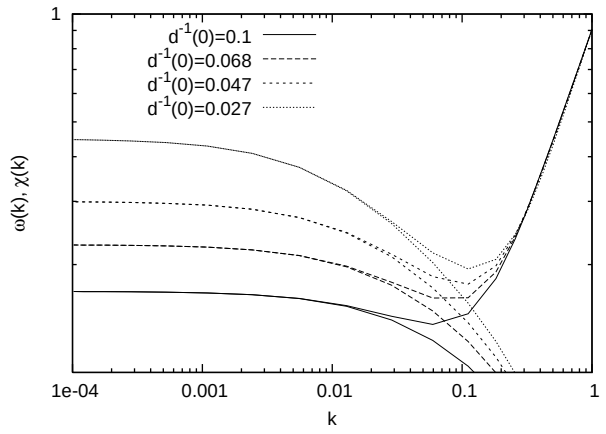

FIG. 11: Infrared part of the plot shown in Fig. 10.

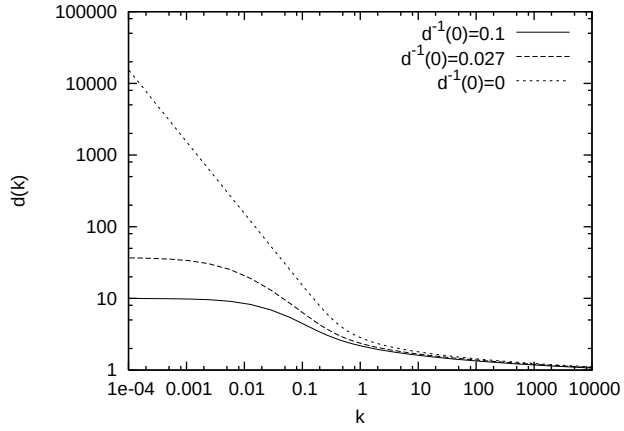

FIG. 12: The ghost form factor $d(k)$, computed as described in the text, together with the result described previously, where the horizon condition is implemented. Note that the Coulomb form factor in the solutions with the horizon condition is computed with the bare value of the ghost form factor, $d \equiv 1$, and thus is not enhanced in the infrared.

B. The search for the critical $f(\mu)$

In a second calculation, $f(\mu)$ was increased to see whether a solution where $f(k)$ becomes infrared divergent ("critical solution") can be found. However, increasing $f(\mu)$ over some specific value produces a system where $\omega(k)$ becomes instable in the infrared. This corresponds to the idea that a critical behaviour leads to the non-availability of a fully consistent solution of the three coupled equations. One can then use an additional degree of freedom that arises when one does not set the finite constants on the right hand sides of the Eqs. (37) and (38) to zero, but instead to some finite values. We rewrite the gap equation as

$$\begin{aligned} \omega^2(k) - \bar{\chi}^2(k) &= k^2 + \xi_0' + \Delta I_\omega^{(2)}(k,0) \\ &+ 2\bar{\chi}(k)\left(\xi + \Delta I_\omega^{(1)}(k,0)\right), \end{aligned} \quad (65)$$

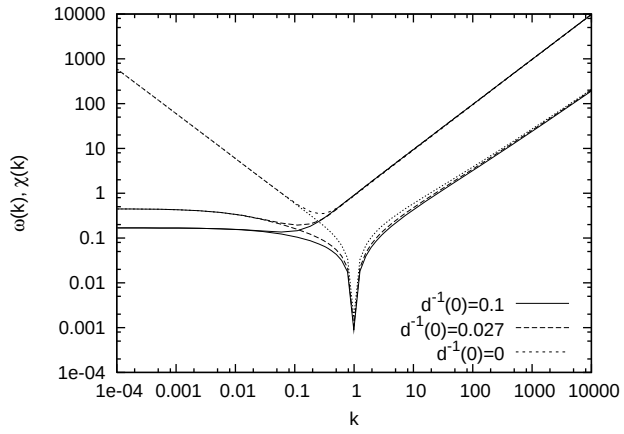

FIG. 13: C.f. Fig. 12, but here shown are the gluon form factor, $\omega(k)$, and the modulus of the scalar curvature, $\chi(k)$.

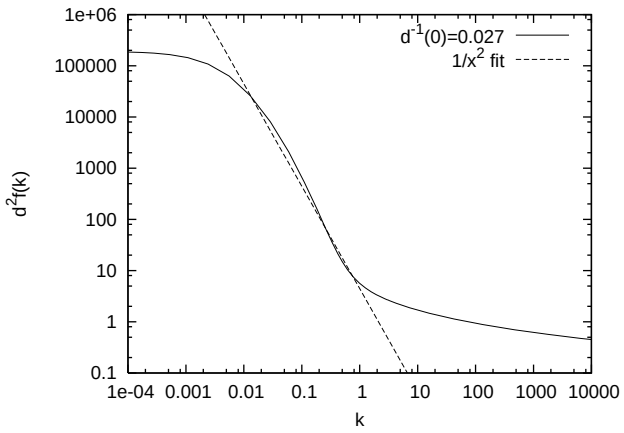

FIG. 14: The product $d^2(k)f(k)$.

where ξ and ξ_0' are finite parameters. Setting these parameters to zero results in the same gap equation (41) as used before. ξ_0' can be used to adjust the value of $\omega(\mu)$. In order to keep the (for the 't Hooft loop desired) IR behavior of $\lim_{k\to 0}(\omega(k) - \bar{\chi}(k)) = 0$, ξ must then assume a certain value,

$$\xi = -\frac{\xi_0'}{2\bar{\chi}(0)}\,. \quad (66)$$

Using this additional degree of freedom of tuning ξ_0', one can effectively increase $\omega(\mu)$, and also the infrared limit $\omega(0)$. This has the effect that the system becomes stable again. However, in the search of the critical $f(\mu)$, this does not help, since the infrared limit of $f(k)$ is decreased by the increased infrared strength of $\omega(k)$.
Fig. 16 illustrates this. We see the solution corresponding to Eq. (41), with $f_\mu = 1$. Increasing f_μ to 2 produces the long dashed line, which shows instabilities in the infrared behaviour of $\omega(k)$. Increasing ξ_0' as well, see the short-dashed line, we get stable solutions again, but with a smaller (non-critical) value of $f(k)$.

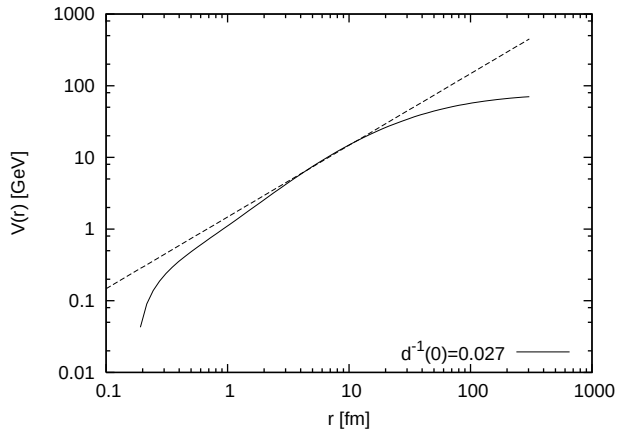

FIG. 15: The static quark potential in coordinate space, $V(r)$.

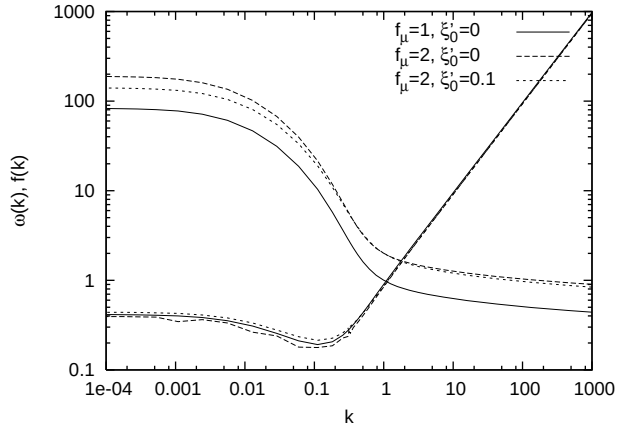

FIG. 16: Solutions for the fully coupled system for different f_μ and ξ_0'.

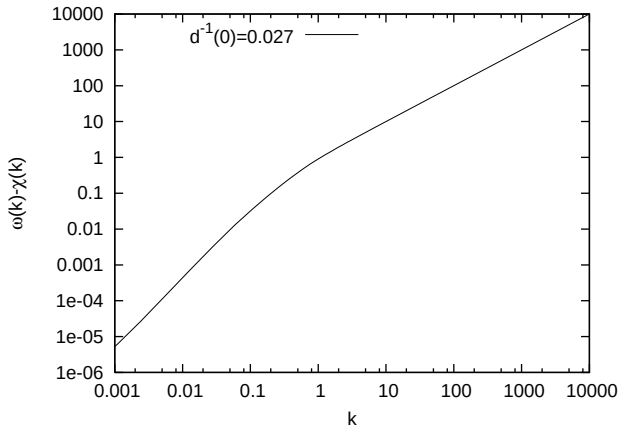

FIG. 17: $\omega(k) - \chi(k)$ log-over-lin plot.

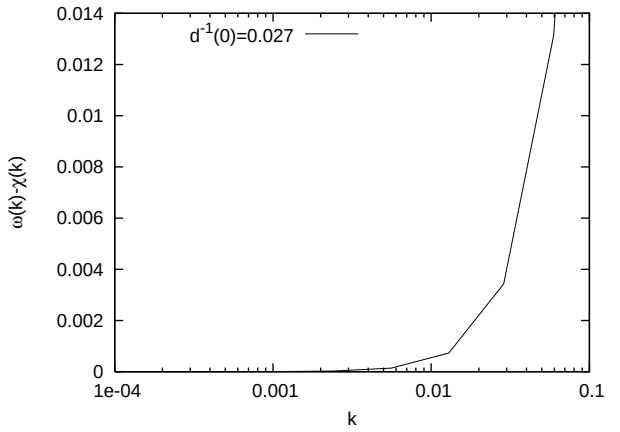

FIG. 18: $\omega(k) - \chi(k)$, lin-over-log plot.

In another calculation, we test the point claimed in the introduction that the Coulomb equation is responsible for the non-availability of solutions of the fully coupled system when the horizon condition is included. To do so, we calculate some initial, infrared-finite $\omega(k)$ as solution of the subcritical system as shown in Fig. 10. We then keep this $\omega(k)$ fixed and solve the system only for $d(k)$ with decreasing d_0^{-1}, and with these $d(k)$ we calculate the corresponding $f(k)$. We find that for every finite d_0^{-1}, both $d(k)$ and $f(k)$ have solutions. With decreasing d_0^{-1}, the $d(k)$ approach a certain asymptotical function. In the critical case where we perform the calculation with the horizon condition, $d_0^{-1} = 0$, the ghost equation still has a solution, and this solution is equal to the limit of the solutions with finite, but decreasing d_0^{-1},

$$\lim_{d_0^{-1}\to 0} d(k; d_0^{-1}) = d(k; d_0^{-1} = 0)\,, \tag{67}$$

with

$$d(k; 0) < \infty \quad \forall\, k > 0. \tag{68}$$

On the other hand, the $f(k)$ become larger and larger with decreasing d_0^{-1}, and an asymptotical function $f(k; d_0^{-1} = 0)$ that is defined similar to (67) does not exist. In the critical case where the horizon condition is implemented, the Coulomb equation has no solution: during the iteration process, the values for $f(k)$ grow larger and larger, without limit, to diverge eventually, representing the fact that the Coulomb equation has no solution in this case. Results of this computations are shown in Figs. 20,21.

Finally, we calculated the 't Hooft loop using the solutions for the form factors presented in this paper. It has been shown in [18] that the large-R-behavior of the 't Hooft loop is determined by the infrared behavior of $\omega(k) - \chi(k)$. We give results for this quantity $\omega(k) - \chi(k)$, and for the 't Hooft loop itself, in Figs. 17-19. If we choose our renormalization constants such that $\omega(k) - \chi(k)$ approaches 0 for $k \to 0$, then the 't Hooft loop goes to a constant for large R, which is in accord with the results given in [18].

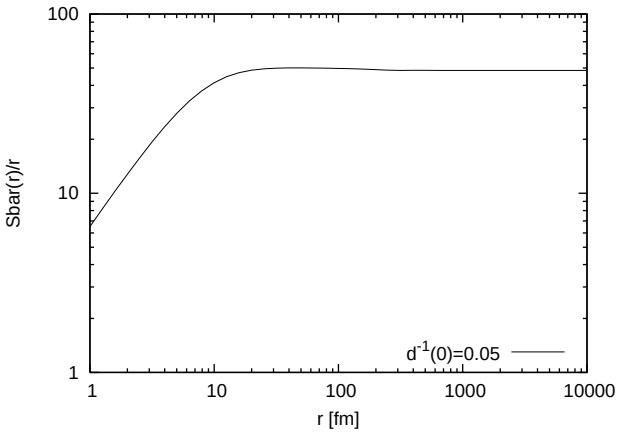

FIG. 19: The renormalized 't Hooft loop exponent $\bar{S}(R)/R$.

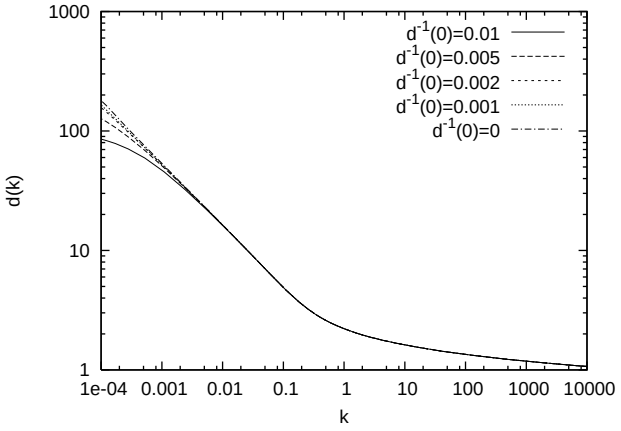

FIG. 20: The ghost form factor for different values of d_0^{-1} calculated with a fixed, infrared-finite $\omega(k)$. We find that this form factor approaches a limit that corresponds to the critical solution with implemented horizon condition.

VI. SUMMARY

A non-perturbative solution to the Yang-Mills Schrödinger equation in Coulomb gauge was presented. As a variational ansatz, a Gaussian type of wave functional was used to minimize the energy. The ultraviolet divergences in the three Dyson-Schwinger equations thus obtained were removed by introduction of appropriate counter terms in the Hamiltonian and in the wave functional. It was shown that within the approximations, no self-consitent solution to all Dyson-Schwinger equations can be found that complies with the horizon condition. Relaxing the horizon condition, on the other hand, we did find a self-consistent solution where all form factors approach finite values in the infrared. This subcritical solution arises if the gauge coupling is chosen to be smaller than some critical value. Approaching this critical value from below, the Coulomb form factor f ceases to solve its DSE. Apparantly, the approximation of the ghost-gluon vertex has a different

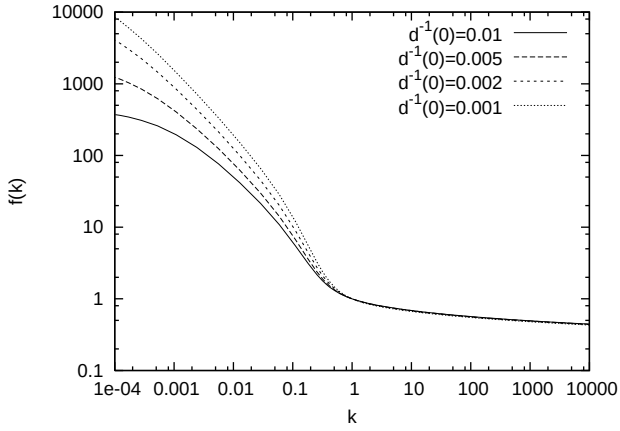

FIG. 21: The Coulomb form factors, calculated with a fixed, infrared-finite $\omega(k)$, and the ghost form factors as shown in Fig. 20. This form factor does not have a limit.

effect on f than it has on d. This explains why in previous calculations, critical solutions were found only if the DSE for f was ignored.

The subcritical solution with infrared finite form factors presented here have some interesting features. First of all, the gluon propagates like massive particle. Secondly, with the ghost and Coulomb form factors d and f being infrared finite, the heavy quark potential can be found to be linear just for a finite range of separation, up to $10fm$. For phenomenological calculations, the use of these form factors may give sensible results, and a further investigation would certainly be interesting.

Acknowledgements

This work was supported by the Deutsche Forschungsgemeinschaft (DFG) under contract no. Re856/6-1,2 and the US Department of Energy under grant DE-FG0287ER40365. The authors are grateful to Axel Weber for valuable discussions. APS would also like to acknowledge the hospitality extend during his visit to Tübingen University where part of this work was completed.

[1] D. R. Thompson *et al.* [E852 Collaboration], Phys. Rev. Lett. **79**, 1630 (1997) [arXiv:hep-ex/9705011].

[2] E. I. Ivanov *et al.* [E852 Collaboration], Phys. Rev. Lett. **86**, 3977 (2001) [arXiv:hep-ex/0101058].

[3] A. P. Szczepaniak, M. Swat, A. R. Dzierba and S. Teige, Phys. Rev. Lett. **91**, 092002 (2003)

[arXiv:hep-ph/0304095].
[4] G. S. Adams *et al.* [E852 Collaboration], Phys. Rev. Lett. **81**, 5760 (1998).
[5] N. H. Christ and T. D. Lee, Phys. Rev. D **22**, 939 (1980) [Phys. Scripta **23**, 970 (1981)].
[6] A. R. Swift, Phys. Rev. D **38** (1988) 668.
[7] D. Schutte, Phys. Rev. D **31** (1985) 810.
[8] R. E. Cutkosky and K. C. Wang, Phys. Rev. D **37**, 3024 (1988).
[9] D. Zwanziger, Phys. Rev. D **69**, 016002 (2004) [arXiv:hep-ph/0303028].
[10] A. P. Szczepaniak and E. S. Swanson, Phys. Rev. D **65**, 025012 (2002) [arXiv:hep-ph/0107078].
[11] A. P. Szczepaniak, Phys. Rev. D **69**, 074031 (2004) [arXiv:hep-ph/0306030].
[12] C. Feuchter and H. Reinhardt, Phys. Rev. D **70**, 105021 (2004) [arXiv:hep-th/0408236], [arXiv:hep-th/0402106].
[13] H. Reinhardt and C. Feuchter, Phys. Rev. D **71**, 105002 (2005) [arXiv:hep-th/0408237].
[14] J. P. Greensite, Nucl. Phys. B **158**, 469 (1979).
[15] J. Greensite and S. Olejnik, arXiv:0707.2860 [hep-lat].
[16] J. Greensite, S. Olejnik and D. Zwanziger, Phys. Rev. D **69**, 074506 (2004) [arXiv:hep-lat/0401003].
[17] J. Greensite and S. Olejnik, Phys. Rev. D **67**, 094503 (2003) [arXiv:hep-lat/0302018].
[18] H. Reinhardt and D. Epple, Phys. Rev. D **76** (2007) 065015 [arXiv:0706.0175 [hep-th]].
[19] W. Schleifenbaum, M. Leder and H. Reinhardt, Phys. Rev. D **73** (2006) 125019 [arXiv:hep-th/0605115].
[20] D. Zwanziger, Phys. Rev. D **65** (2002) 094039 [arXiv:hep-th/0109224].
[21] D. Epple, H. Reinhardt and W. Schleifenbaum, Phys. Rev. D **75** (2007) 045011 [arXiv:hep-th/0612241].
[22] K. Langfeld and L. Moyaerts, Phys. Rev. D **70** (2004) 074507 [arXiv:hep-lat/0406024].
[23] C. Feuchter and H. Reinhardt, arXiv:0711.2452 [hep-th].
[24] L. Moyaerts, PhD thesis, Univ. of Tübingen (2004).